



Capillary electrophoresis as sample introduction system for highly sensitive and interference-free determination of ^{99}Tc by ICP-MS

Dan Zhou^{a,c}, Liangjin Bao^b, Haoqi Long^b, Duo Zhou^b, Yuwei Xu^b, Bo Wang^b,
Chuanqin Xia^a, Liang Xian^{b,*}, Chengbin Zheng^{a,*}

^a Key Laboratory of Green Chemistry & Technology of MOE, College of Chemistry, Sichuan University, Chengdu 610064, China

^b Department of Radiochemistry, China Institute of Atomic Energy, Beijing 102413, China

^c State Key Laboratory of Radiation Medicine and Protection, School of Radiation Medicine and Protection, Collaborative Innovation Center of Radiological Medicine of Jiangsu Higher Education Institutions, Soochow University, Suzhou 215123, China

ARTICLE INFO

Article history:

Received 29 January 2024

Revised 23 May 2024

Accepted 5 June 2024

Available online 5 June 2024

Keywords:

Radionuclide technetium-99

Capillary electrophoresis-inductively coupled plasma mass spectrometry (CE-ICP-MS)

Rhenium (Re)

Interference-free determination

ABSTRACT

Although inductively coupled plasma mass spectrometry (ICP-MS) retains high sensitivity and has been intensively used for the measurement of ^{99}Tc , it usually suffers from tedious, expensive, and time-consuming sample pretreatments due to the isobaric interferences from ^{99}Ru and $^{98}\text{Mo}^1\text{H}$. Herein, capillary electrophoresis (CE) was applied as sample introduction system for the sensitive, and interference-free determination of $^{99}\text{TcO}_4^-$ from RuO_4^- , and MoO_4^{2-} by ICP-MS with a simple sample treatment. Compared to the conventional methods, the hyphenated CE-ICP-MS avoids the use of expensive separation resins and reduces the consumption of mineral acid, representing a simpler, more efficient and environmentally benign approach. Moreover, the proposed method exhibits higher accuracy compared with the mathematical correction method using the natural isotope ratio of ^{99}Ru and ^{101}Ru , and significantly reduces sample consumption and the amount of waste, thus remarkably alleviating the radioactive exposure to operators and the pressure of radioactive waste treatment. Under the optimized conditions, the detection limits of 25 $\mu\text{g/L}$ and 0.06 $\mu\text{g/L}$ were obtained for RuO_4^- and ReO_4^- (Tc was replaced by Re), respectively, with relative standard deviation (RSD) lower than 5%. In addition, efficient recoveries of RuO_4^- , ReO_4^- , and $^{99}\text{TcO}_4^-$ from simulated Hanford site groundwater were achieved. The method is expected to be a promising candidate for sensitive and accurate analysis of ^{99}Tc from contaminated environmental samples.

© 2025 Published by Elsevier B.V. on behalf of Chinese Chemical Society and Institute of Materia Medica, Chinese Academy of Medical Sciences.

Technetium-99 (^{99}Tc) is a potential long-lived environmental hazard with a half-life of 2.1×10^5 years. Almost all the ^{99}Tc in the environment results from anthropogenic nuclear activity, including nuclear accidents, nuclear weapon testing, leakage from nuclear power plants, geological disposal, and nuclear medical application of $^{99\text{m}}\text{Tc}$ [1–4]. Following its release, ^{99}Tc will spread through atmospheric deposition, water circulation, and the food chain, leading to a serious threat to humans and other animals and plants [4–9]. Therefore, it is important to accurately and rapidly determine ^{99}Tc in nuclear waste and the environment.

As a pure β -emitter, ^{99}Tc can be measured by radiometric techniques, including gas flow Geiger-Müller (GM) counter [10], liquid scintillation counter (LSC) [11], neutron activation analysis

(NAA) [12,13], and mass spectrometric techniques such as inductively coupled plasma mass spectrometry (ICP-MS) [14–18], resonance ionization mass spectrometry (RIMS) [19], thermal ionization mass spectrometry (TIMS) [20,21], and accelerator mass spectrometry (AMS) [22]. Compared to other methods, ICP-MS simultaneously provides better detection of limit (LOD) and retains the merits of easier access that lowers its instrumentation and operation cost, thus becoming the most used technique for the determination of ^{99}Tc in various samples, especially for environmental samples with complicated components [23–25]. Isobaric interferences from the stable isotope ^{99}Ru and the molecular ion $^{98}\text{Mo}^1\text{H}$ are the main interferences as ICP-MS is used to determine ^{99}Tc . To alleviate these interferences, various separation methods were employed to separate TcO_4^- , RuO_4^- , and MoO_4^{2-} prior to their analyses [15,26–31]. However, these approaches require expensive resin materials and use a large amount of high-concentration strong acid as eluent, which is not only laborious and time-consuming, but also generates a lot of radioactive waste. To reduce the radiolog-

* Corresponding authors.

E-mail addresses: 13552063239@139.com (L. Xian), abinscu@scu.edu.cn (C. Zheng).

ical exposure to operators, several improved techniques integrating automated analysis module into ICP-MS were proposed in recent years [32–37]. In fact, even the methods using resin material were still not capable of completely separating TcO_4^- from RuO_4^- , and MoO_4^{2-} [38,39], causing an inevitable error in the measurement of ^{99}Tc . Thus, a mathematical correction method was developed to correct the concentration of ^{99}Tc based on the natural isotope ratio of $^{99}\text{Ru}/^{101}\text{Ru}$ [15,25,31,40]. However, ^{99}Tc will decay into ^{99}Ru and then the concentration of ^{99}Ru and ^{101}Ru in nuclear waste or the environment are no longer the same as the natural abundance. Therefore, the mathematical correction method cannot accurately correct the concentration of ^{99}Tc [4]. In general, the current ICP-MS methods using resin more or less suffer from inaccuracy on the determination of ^{99}Tc . As a result, it is still a great challenge to develop a sensitive method for the accurate determination of ^{99}Tc without the interferences from ^{99}Ru and $^{98}\text{Mo}^{1}\text{H}$.

Capillary electrophoresis (CE) is a state-of-the-art separation technique and has been widely used for the separations and analyses of radioactive elements [34,41–44]. Owing to its advantages of effective separation, fast analysis speed, and small injection volume, the automated CE not only enables high sample throughput but also reduces the radioactive exposure to operators. Although the CE based techniques have been intensively explored for radioactive elements detection [45–47], they are usually coupled with an ultraviolet and visible spectrophotometry (CE-UV-Vis) detector and then hinder their practical application because of their low sensitivities resulted from low sample injection volume (nL level) and the extremely short optical path. Therefore, it is essential to combine CE with other more sensitive detectors for the determination of ^{99}Tc . Over the past several decades, ICP-MS has been frequently used as a CE detector for the detection or speciation analysis of radioactive elements due to its high sensitivity and elemental specific selectivity [41–43,48–50]. However, to the best of our knowledge, the use of CE as an effective alternative to the conventional resin-based separation methods to eliminate the interferences of ^{99}Ru and $^{98}\text{Mo}^{1}\text{H}$ has never been reported.

In this work, we developed a new automated method coupling CE and ICP-MS for the sensitive and accurate determination of ^{99}Tc . $^{99}\text{TcO}_4^-$ can be completely separated from RuO_4^- and MoO_4^{2-} prior to its determination, thus effectively reducing the isobaric interferences of ^{99}Ru and $^{98}\text{Mo}^{1}\text{H}$. TcO_4^- was replaced by ReO_4^- due to their similar physicochemical properties and electrophoretic behavior [47,51,52]. The developed method avoids the use of expensive resin and the subsequent cumbersome elution process, thus decreasing the analysis cost and reducing the amount of radioactive waste. In addition, the use of hyphenated CE-ICP-MS not only achieves better LODs and consumes less amount of sample compared to conventional methods but also realizes automatic operation, alleviating the radioactive exposure to operators.

The main purpose of this experiment is to eliminate the isobaric interferences on the determination of ^{99}Tc . As a consequence, the initial experiment was to investigate that the feasibility of CE-ICP-MS on the separation and analysis of TcO_4^- , RuO_4^- , and MoO_4^{2-} . Since the conditions for radioactive experiment is limited in Sichuan University, ReO_4^- was thus used as substitutes analogous to TcO_4^- because of their similar physicochemical properties and electro-phoretic behavior. The schematic of the CE-ICP-MS system and the typical running parameters for non-radioactive experiments in Sichuan University are shown in Fig. S1 and Table S1 (Supporting information). According to previous work [47,53,54], a buffer solution containing 10 mmol/L K_2CO_3 (pH 11.0) was firstly used to separate and analyze KReO_4 , KRuO_4 , and K_2MoO_4 by CE-ICP-MS. The results summarized in Fig. S2 (Supporting information) show that the isolated signals for ReO_4^- and RuO_4^- can be clearly observed, whereas no signal is detected for MoO_4^{2-} even the separation time longer than 40 min. This is probably because

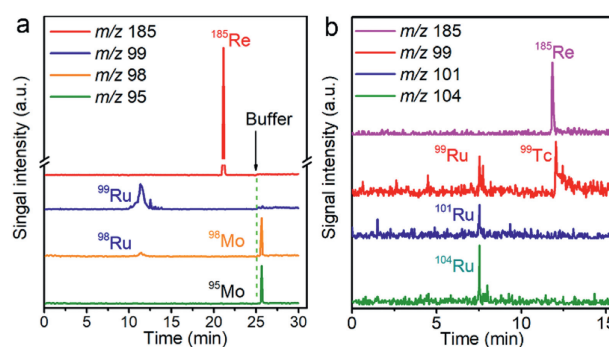


Fig. 1. The electropherograms of (a) 348 $\mu\text{g/L}$ K_2MoO_4 , 3.33 mg/L KRuO_4 , and 33.3 $\mu\text{g/L}$ KReO_4 mixture using 10 mmol/L K_2CO_3 solution as buffer solution and washing fluid, (b) 100 $\mu\text{g/L}$ KReO_4 , 100 $\mu\text{g/L}$ $\text{NH}_4^{99}\text{TcO}_4$, and 5 mg/L KRuO_4 mixture.

that MoO_4^{2-} cannot be eluted from the capillary under this operating condition. Subsequently, we applied the pressure-assisted introduction of buffer solution to swept the compounds kept in the capillary into the ICP-MS after appearing the signals of ReO_4^- and RuO_4^- . Interestingly, the signals for ^{98}Mo and ^{95}Mo were detected besides of the signals for Re and Ru (Fig. 1a), confirming the aforementioned speculation and the feasibility of the CE-ICP-MS on the separation and analysis of ReO_4^- from RuO_4^- and MoO_4^{2-} .

To further study the interference of $^{98}\text{Mo}^{1}\text{H}$ at $m/z = 99$, various concentrations of MoO_4^{2-} (0.001, 0.01, 0.1, 1, and 10 mg/L) were added into the standard solution of RuO_4^- and then analyzed by ICP-MS using no gas mode and He mode. Although ^{98}Mo signal was increased with increasing the concentration of MoO_4^{2-} , the ^{99}Ru signal kept stable regardless that the no gas mode or He mode was used (Fig. S3 in Supporting information), suggesting that the interference from MoO_4^{2-} was negligible on the determination of TcO_4^- . A comparison between the results obtained under the no gas mode and He mode, which suggests the latter is a better choice because a smaller relative standard deviation (RSD) is achieved, so He mode and 10 mmol/L K_2CO_3 (pH 11.0) buffer are selected for the subsequent experiments.

In order to demonstrate that the CE-ICP-MS system can accomplish the sensitive and interference-free determination of ^{99}Tc from RuO_4^- , a mixture containing 100 $\mu\text{g/L}$ KReO_4 , 100 $\mu\text{g/L}$ $\text{NH}_4^{99}\text{TcO}_4$, and 5 mg/L KRuO_4 was analyzed. The typical running parameters of CE-ICP-MS were listed in Table S2 (Supporting information). As shown in Fig. 1b, TcO_4^- and RuO_4^- retain different migration time, which evidently demonstrates the feasibility of the successful and complete separation and analysis of TcO_4^- from RuO_4^- . Therefore, the isobaric interference of ^{99}Ru on the determination of ^{99}Tc can be efficiently eliminated by CE-ICP-MS. Most importantly, Fig. 1b shows that ReO_4^- provides same migration time with ^{99}Tc , which verifies the similar electrophoretic behavior between Tc and Re . Therefore, ReO_4^- can be used as a stable substitute analogous to TcO_4^- and used in the subsequent experiments.

To achieve the optimal analytical performance for the separation of ReO_4^- and RuO_4^- , different parameters that affected the separation efficiency of CE-ICP-MS were initially optimized. The length of the capillary plays an important role in the separation efficiency and then FS-capillaries with length of 97 cm and 108 cm were conducted to explore their performances on the separation of RuO_4^- and ReO_4^- . From Fig. S4 (Supporting information), it showed that both these two FS-capillaries can achieve the complete separation of RuO_4^- and ReO_4^- , while a shorter FS-capillary can significantly save the analysis time. Thus, the FS-capillary of length of 97 cm was used in the subsequent experiments. The concentration of buffer directly affected the ionic strength of the electrophoretic medium, which further influenced the zeta potential and the electroosmotic flow (EOF). The concentrations of K_2CO_3

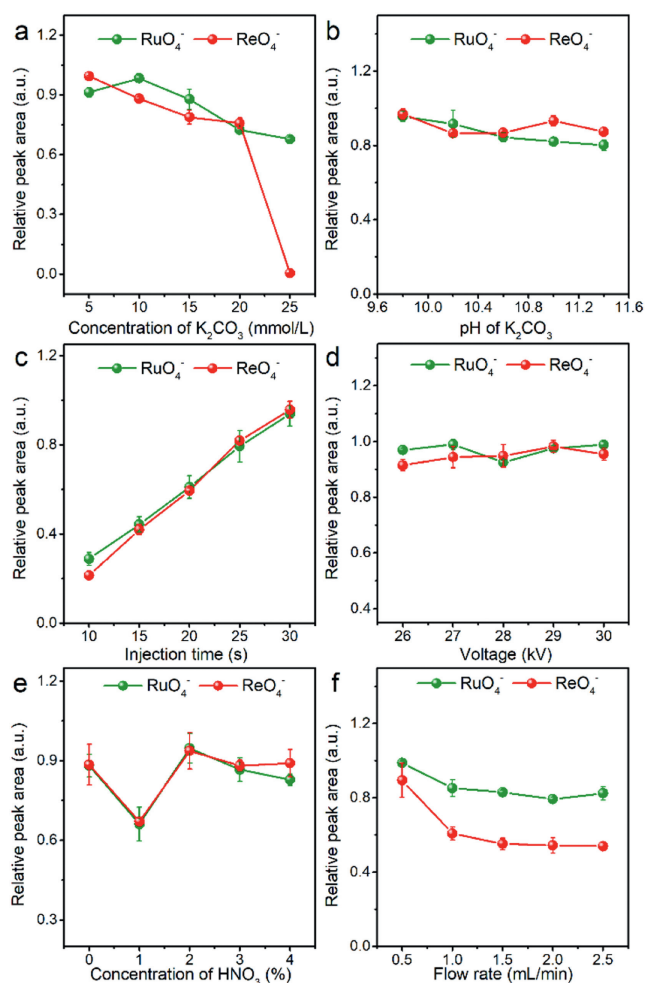


Fig. 2. The effect of (a) buffer concentration, (b) pH of buffer, (c) injection time of sample, (d) separation voltage, (e) different HNO₃ concentration as sheath fluid, and (f) different HNO₃ flow rates on separation efficiency with 100 μg/L KReO₄ and 5 mg/L KRuO₄ mixture.

ranging from 5–25 mmol/L was investigated. Fig. 2a shows that the peak area of RuO₄⁻ increased as the buffer concentration increased from 5 mmol/L to 10 mmol/L and achieved the top at the buffer concentration of 10 mmol/L. The peak area of ReO₄⁻ decreased as the buffer concentration increased. The migration time of RuO₄⁻ and ReO₄⁻ prolonged with the increase of buffer concentration and could not obtain the signal of Re at the buffer concentration of 25 mmol/L (Fig. S5 in Supporting information). The buffer capacity increases with the increase of concentration of the buffer solution, ensuring that the pH and conductivity of the local separation buffer solution will not change at the moment of sample injection. However, excessively high salt concentration will generate more Joule heat reducing the separation efficiency of RuO₄⁻ and ReO₄⁻ and even could not obtain the signal of Re [55]. In addition, the high concentration of buffer solution also leads to the low nebulization efficiency of ICP-MS [56]. Therefore, 10 mmol/L of K₂CO₃ concentration was selected in the subsequent experiments.

The pH of the buffer system directly affects the degree of protonation of the silanol group in the capillary wall, which further affects the EOF and separation efficiency of RuO₄⁻ and ReO₄⁻. Consequently, we studied the pH in the range of 9.8–11.4 by adding appropriate amounts of 1 mol/L HCl or NaOH. As shown in Fig. 2b, the peak area of RuO₄⁻ decreased with the increase of buffer pH. However, the peak area of ReO₄⁻ decreased as the buffer pH increased from 9.8 to 10.2, 11.0 to 11.4, and achieved the top at pH

11.0. The EOF increased with the increase of buffer pH, generating more Joule heat and reducing the peak areas of RuO₄⁻ and ReO₄⁻. Buffer pH also affects the dissociation ability of samples and different samples need different separation pH, which might cause the increased peak area of ReO₄⁻ at pH 11.0. Considering the separation efficiency of RuO₄⁻ and ReO₄⁻, pH 11.0 of K₂CO₃ buffer solution was preferred in subsequent experiments. The injection time is positively correlated with the injection volume under the hydrodynamic injection mode, thus, different injection times (10, 15, 20, 25, and 30 s) were tested. The peak areas of RuO₄⁻ and ReO₄⁻ gradually increased with the increase of the injection time in the range of 10–30 s (Fig. 2c). However, the peak of RuO₄⁻ became broader with the increase of injection time of samples (Fig. S6 in Supporting information). The ionic strength of the solution increased with the amount of sample increased, which will reduce the accumulation effect of electric field focusing and reduce the separation efficiency [57]. Furthermore, too long injection time would induce the overloaded of sample with the increase of sample concentration, causing the decrease of separation efficiency. Thus, the injection time of 20 s was selected in this work.

The separation voltage of CE was also optimized on account of its influence on separation efficiency and field strength. As shown in Fig. 2d, five different voltages (26, 27, 28, 29, and 30 kV) were investigated. The achieved peak area of RuO₄⁻ increased from 26 kV to 27 kV, 28 kV to 30 kV, and with the highest peak area at 27 kV. Nevertheless, the achieved peak area of ReO₄⁻ increased from 26 kV to 29 kV, and achieved the highest peak area at 29 kV. According to the corresponding diagram of the working current and separation voltage, the curve bends at the separation voltage of 28 kV (Fig. S7 in Supporting information), and the Joule heat could not be effectively dissipated at this time. The Joule heat increased with the increase of separation voltage, reducing the separation efficiency of RuO₄⁻ and ReO₄⁻ [58,59]. To obtain a higher theoretical plate number, a voltage in the linear range should be used during the CE separation process. Therefore, the separation voltage was chosen at 27 kV.

The composition of the sheath fluid significantly affects the nebulized efficiency at the end of the CE capillary, thus affecting the sample introduction efficiency and analytical performance. Thus, different concentrations of sheath fluid (HNO₃) and the flowrate of sheath fluid on the intensities of Re and Ru were investigated in a range of 0%–4% (v/v). Fig. S8a (Supporting information) shows that both DIW and different concentrations of HNO₃ can achieve high signal-to-noise ratios of RuO₄⁻ and ReO₄⁻, the corresponding peak area concluded in Fig. 2e. The peak area of RuO₄⁻ decreased with HNO₃ concentration in the range of 0%–1% and 2%–4%, and achieved the top at the HNO₃ concentration of 2%. The peak area of ReO₄⁻ decreased with concentration of HNO₃ increased from 0% to 1%, 2% to 3%, and increased with the concentration of HNO₃ increased from 1% to 2%, 3% to 4%. The highest peak area of RuO₄⁻ and ReO₄⁻ both at the HNO₃ concentration of 2%. A stable CE current is a precondition for utilization, from Fig. S8b (Supporting information), it can be observed that all the HNO₃ solutions maintain stability except for DIW. Thus, 2% (v/v) HNO₃ was selected as the sheath fluid. Fig. 2f shows that the peak areas of both RuO₄⁻ and ReO₄⁻ decreased with the flow rate increased from 0.5 mL/min to 1.0 mL/min, and become stable after the flow rate of 1.0 mL/min. To obtain excellent sensitivity, we chose the sheath fluid flowrate at 1.0 mL/min. It is worth noting that the electrophoretic migration time gradually prolonged over time, which may be owing to the carbon dioxide absorption from the air and changed the thickness of the electric double layer.

Under the optimal conditions, analytical figures of merit using CE-ICP-MS were evaluated by analyzing a series of standard solutions with various concentrations of KReO₄ (0, 1, 2, 5, 10, 20, 50, 100, and 200 μg/L) containing different concentrations of

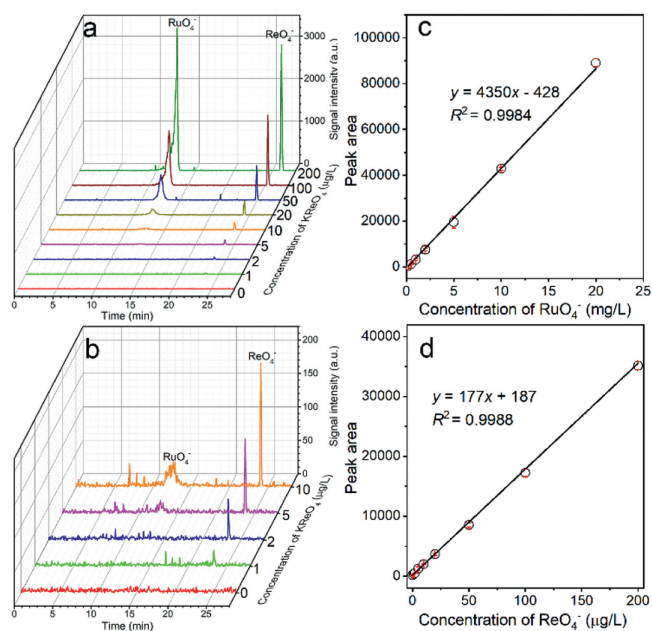


Fig. 3. (a) The electropherograms of RuO₄⁻ and ReO₄⁻ with various concentrations of KReO₄ from (a) 1–200 μg/L and (b) 1–10 μg/L, and corresponding typical calibration curves of (c) RuO₄⁻ and (d) ReO₄⁻, respectively.

KRuO₄ (0, 0.1, 0.2, 0.5, 1, 2, 5, 10, and 20 mg/L). The electropherograms of RuO₄⁻ and ReO₄⁻ are shown in Figs. 3a and b, which show the gradually increased peaks of RuO₄⁻ from 0.2 mg/L to 20 mg/L, and ReO₄⁻ from 1 μg/L to 200 μg/L, respectively. Figs. 3c and d show the corresponding typical calibration curves of RuO₄⁻ and ReO₄⁻, respectively. The linear correlation coefficients (R^2) are better than 0.99 for these calibration curves, which retain linear ranges of 0.2–20 mg/L for RuO₄⁻ and 1–200 μg/L for ReO₄⁻, respectively. The LODs, defined as the analyte concentration equivalent to 3 times the standard deviation of 11 measurements of a blank solution (DIW) divided by the slope of the calibration curve, were 0.025 mg/L for RuO₄⁻ and 0.06 μg/L for ReO₄⁻, respectively. The LOD of ReO₄⁻ is much lower than that of CE-UV method, but higher than that of other ICP-MS methods due to small volume of sample injection (Table S3 in Supporting information). However, the LOD is not the most significant advantage of the proposed CE-ICP-MS. Compared to other ICP-MS methods, the present method coupled CE, the separation end, with ICP-MS, the quantified detection end. This integration on the one hand sacrifices the LOD to some extent, but on the other achieves the suppression of interference from ⁹⁹Ru, which is not achievable by other ICP-MS methods. The precision is expressed as the RSD of five replicate measurements, yielding values of 4.6% and 4.3% for RuO₄⁻ and ReO₄⁻, respectively (Fig. S9 in Supporting information).

To verify the accuracy and practicability of the proposed method, Hanford site groundwater samples were simulated according to a reported protocol by adding various concentrations of KReO₄ (0, 0.6, 6, 60, and 100 μg/L), KRuO₄ (0, 60, 600, 6000, 10,000 μg/L), and NH₄⁹⁹TcO₄ (0, 0.6, 6, 60, and 100 μg/L), respectively [54]. The ingredient of Hanford site groundwater listed in Table S4 (Supporting information). The electropherograms of simulated Hanford site groundwater samples spiked with different concentrations of KRuO₄, KReO₄, and NH₄⁹⁹TcO₄ are shown in Figs. S10a and b (Supporting information). The obtained results show that the signals of RuO₄⁻, ReO₄⁻, and ⁹⁹TcO₄⁻ were successfully observed. The analysis time of per simulated Hanford site groundwater samples spiked with different concentrations of NH₄⁹⁹TcO₄ were in 20 min including the capillary rinsed with running buffer

solution for 2 min. Table S5 (Supporting information) lists the recovery rates for the samples spiked with different concentrations of KRuO₄, KReO₄, and NH₄⁹⁹TcO₄, showing that good recovery ranging from 85.6%–96.7% were obtained by the proposed analytical systems. The analytical results confirm the accuracy and practicability of the proposed method, which is expected to be used for highly sensitive and accurate determination of actual samples contaminated by ⁹⁹Ru and ⁹⁹Tc with ICP-MS.

In this work, the separation and detection of ⁹⁹TcO₄⁻ from RuO₄⁻, and MoO₄²⁻ were achieved by using CE as a sampling system for ICP-MS. To obtain high sensitivity and reduce the radiological exposure to operators, ReO₄⁻ was used as the analogue of ⁹⁹TcO₄⁻. The proposed method is more accurate compared with the mathematical correction method using the natural isotope ratio of ⁹⁹Ru and ¹⁰¹Ru. In addition, the proposed method avoided the use of expensive resin materials and a large amount of high-concentration strong acid, which can save the analysis cost and is more friendly to the environment. Most importantly, the hyphenated CE-ICP-MS holds superiority not only in requiring a small volume of sample for low LODs and automated operation, which significantly reduces the radiological exposure to operators. The automated method is expected to be a promising candidate for sensitive and accurate analysis of ⁹⁹Tc contaminated environmental samples by ICP-MS.

Declaration of competing interest

We declare that there are no financial and personal relationships with other people or organizations that can inappropriately influence our work, there is no professional or other personal interest of any nature or kind in any product, service and/or company that could be construed as influencing the position presented in, or the review of, the manuscript entitled.

CRediT authorship contribution statement

Dan Zhou: Conceptualization, Data curation, Formal analysis, Investigation, Methodology, Writing – original draft, Writing – review & editing. **Liangjin Bao:** Investigation, Resources, Writing – review & editing. **Haoqi Long:** Investigation, Resources, Writing – review & editing. **Duo Zhou:** Funding acquisition, Investigation, Writing – review & editing. **Yuwei Xu:** Investigation, Resources, Writing – review & editing. **Bo Wang:** Data curation, Formal analysis, Investigation, Writing – review & editing. **Chuanqin Xia:** Funding acquisition, Writing – review & editing, Resources. **Liang Xian:** Investigation, Resources, Writing – review & editing. **Chengbin Zheng:** Conceptualization, Data curation, Formal analysis, Funding acquisition, Investigation, Methodology, Project administration, Resources, Supervision, Writing – review & editing.

Acknowledgments

The authors gratefully acknowledge the National Natural Science Foundation of China (Nos. U1867205, 21622508, and 21575092) and Study on Physical/Chemical Characteristics Related to the Migration of Key Nuclides under Simulated Disposal Conditions (Phase II) (Contract No. KGES 2019(170), dated February 21, 2019.) for financial support.

Supplementary materials

Supplementary material associated with this article can be found, in the online version, at doi:10.1016/j.ccl.2024.110093.

References

- [1] M. García-León, J. Nucl. Radiochem. Sci. 6 (2005) 253–259.
- [2] A.H. Meena, Y. Arai, Environ. Chem. Lett. 15 (2017) 241–263.
- [3] J.P. Icenhower, N.P. Qafoku, J.M. Zachara, W.J. Martin, Am. J. Sci. 310 (2010) 721–752.
- [4] K.L. Shi, X.L. Hou, P. Roos, W.S. Wu, Anal. Chim. Acta 709 (2012) 1–20.
- [5] H. Ji, Y. Zhu, J. Duan, et al., Chin. Chem. Lett. 30 (2019) 2163–2168.
- [6] K.L. Shi, X.L. Hou, P. Roos, W.S. Wu, Anal. Chem. 84 (2012) 2009–2016.
- [7] S.M. Keogh, A. Aldahan, G. Possnert, et al., J. Environ. Radioact. 95 (2007) 23–38.
- [8] E.H. Schulte, P. Scoppa, Sci. Total Environ. 64 (1987) 163–179.
- [9] D.M. LaSage, A.E. Fryar, A. Mukherjee, N.C. Sturchio, L.J. Heraty, J. Hydrol. 360 (2008) 265–280.
- [10] Q.J. Chen, H. Dahlgaard, H.J.M. Hansen, A. Aarkrog, Anal. Chim. Acta 228 (1990) 163–167.
- [11] F. Wigley, P.E. Warwick, I.W. Croudace, J. Caborn, A.L. Sanchez, Anal. Chim. Acta 380 (1999) 73–82.
- [12] S. Foti, E. Delucchi, V. Akamian, Anal. Chim. Acta 60 (1972) 269–276.
- [13] X.L. Hou, P. Roos, Anal. Chim. Acta 608 (2008) 105–139.
- [14] K. Tagami, S. Uchida, T. Hamilton, W. Robison, Appl. Radiat. Isot. 53 (2000) 75–79.
- [15] L. Skipperud, D.H. Oughton, L.S. Rosten, et al., J. Environ. Radioact. 98 (2007) 251–263.
- [16] L. Yang, W.T. Bu, K. Xiong, Y.Q. Yang, T.Z. Yang, Spectrochim. Acta B 198 (2022) 106564.
- [17] B.C. Russell, P.E. Warwick, H. Mohamud, et al., J. Anal. At. Spectrom. 38 (2023) 97–110.
- [18] W.T. Bu, L. Yang, L. Tang, et al., J. Anal. At. Spectrom. 37 (2022) 1174–1178.
- [19] S.W. Downey, N.S. Nogar, C.M. Miller, Int. J. Mass Spectrom. Ion Process 61 (1984) 337–345.
- [20] L.X. Wang, L. Tang, T.Z. Yang, Y.Q. Yang, L. Yang, J. Radioanal. Nucl. Chem. 296 (2013) 739–742.
- [21] P. Dixon, D.B. Curtis, J. Musgrave, et al., Anal. Chem. 69 (1997) 1692–1699.
- [22] B.A. Bergquist, A.A. Marchetti, R.E. Martinelli, et al., Nucl. Instrum. Meth. Phys. Res. B 172 (2000) 328–332.
- [23] K.L. Shi, X.L. Hou, J.X. Qiao, et al., Anal. Chem. 88 (2016) 11931–11937.
- [24] M.A. French, H. Zhang, J.M. Pates, S.E. Bryan, R.C. Wilson, Anal. Chem. 77 (2005) 135–139.
- [25] J.M. Más, M. García-León, J.P. Bolívar, Nucl. Instrum. Meth. Phys. Res. A 484 (2002) 660–667.
- [26] J.H. Chao, C.L. Tseng, C.J. Lee, J. Radioanal. Nucl. Chem. 251 (2002) 105–112.
- [27] J.C. Butterworth, F.R. Livens, P.R. Makinson, Sci. Total Environ. 173/174 (1995) 293–300.
- [28] J.L. Mas, M. García-León, J.P. Bolívar, Appl. Radiat. Isot. 64 (2006) 502–507.
- [29] C.S. Dileep, P. Jagasia, P.S. Dhani, et al., Desalination 232 (2008) 157–165.
- [30] S.B. Jenkinson, D. McCubbin, P.H.W. Kennedy, et al., J. Environ. Radioact. 133 (2014) 40–47.
- [31] H. Sahli, S. Röllin, J.A.C. Alvarado, J. Radioanal. Nucl. Chem. 311 (2017) 1633–1642.
- [32] K.L. Shi, J.X. Qiao, W.S. Wu, P. Roos, X.L. Hou, Anal. Chem. 84 (2012) 6783–6789.
- [33] K. Kolaćńska, M. Trojanowicz, Talanta 125 (2014) 131–145.
- [34] Y. Jiang, M.Y. He, W.J. Zhang, et al., Chin. Chem. Lett. 28 (2017) 1640–1652.
- [35] R. Rodríguez, L. Leal, S. Miranda, et al., Talanta 133 (2015) 88–93.
- [36] S. Walas, K. Kleszcz, A. Tobiasz, H. Mrowiec, J.W. Mietelski, Anal. Lett. 49 (2016) 2755–2765.
- [37] M. Matsuuda, K. Yanagisawa, K. Koarai, et al., ACS Omega 6 (2021) 19281–19290.
- [38] C.K. Kim, C.S. Kim, B.H. Rho, J.I. Lee, J. Radioanal. Nucl. Chem. 252 (2002) 421–427.
- [39] O. Egorov, M.J. O'Hara, J. Ruzicka, J.W. Grate, Anal. Chem. 70 (1998) 977–984.
- [40] S. Díez-Fernández, H. Isnard, A. Nonell, C. Bresson, F. Chartier, J. Anal. At. Spectrom. 35 (2020) 2793–2819.
- [41] C. Willberger, D. Leichtfuß, S. Amayri, T. Reich, Inorg. Chem. 58 (2019) 4851–4858.
- [42] C. Willberger, S. Amayri, V. Haußler, R. Scholze, T. Reic, Anal. Chem. 91 (2019) 11537–11543.
- [43] L. Li, X.Q. Xue, H.G. Zhang, et al., Chin. Chem. Lett. 32 (2021) 2139–2142.
- [44] X.L. Liu, F. Poineau, M. Fattahi, B. Grambow, L. Vichot, Radiochim. Acta 93 (2005) 305–309.
- [45] T. Haraga, K. Ouchi, Y. Sato, et al., Anal. Chim. Acta 1032 (2018) 188–196.
- [46] E. Ianovici, M. Kosinski, P. Lerch, A.G. Maddoc, J. Radioanal. Chem. 64 (1981) 315–326.
- [47] B. Fourest, A. Maslennikov, F. David, M. Masson, Radiochim. Acta 91 (2003) 479–485.
- [48] E.W. Mei, H. Ichihashi, W.F. Gu, S. Yamasaki, Anal. Chem. 69 (1997) 2187–2192.
- [49] G. Álvarez-Llamas, M.D.R.F.D. laCampa, A. Sanz-Medel, Trends Analyt. Chem. 24 (2005) 28–36.
- [50] J.W. Olesik, J.A. Kinzer, S.V. Olesik, Anal. Chem. 67 (1995) 1–12.
- [51] E.A. Katayev, G.V. Kolesnikov, J.L. Sessler, Chem. Soc. Rev. 38 (2009) 1572–1586.
- [52] D. Banerjee, D. Kim, M.J. Schweiger, A.A. Krugerc, P.K. Thallapally, Chem. Soc. Rev. 45 (2016) 2724–2739.
- [53] E.A. EL-Ghany, F.F. Attia, F. Marzouk, M.T. EL-Kolaly, J. Radioanal. Nucl. Chem. 245 (2000) 237–242.
- [54] D. Zhou, Y. Lin, H.Q. Long, et al., Spectrochim. Acta B 180 (2021) 106211.
- [55] I.I. Stewart, J.W. Olesik, J. Chromatogr. A 872 (2000) 227–246.
- [56] L.H. Liu, Z.J. Yun, B. He, G.B. Jiang, Anal. Chem. 86 (2014) 8167–8175.
- [57] Z.K. Shihabi, J. Chromatogr. A 902 (2000) 107–117.
- [58] S.R. Wallenborg, L. Nyholm, C.E. Lunte, Anal. Chem. 71 (1999) 544–549.
- [59] X.F. Guo, Z.H. Wang, S.P. Zhou, Talanta 64 (2004) 135–139.